

Evacuation Zone Modeling under Climate Change: A Data-Driven Method

Kun Xie, Kaan Ozbay, Yuan Zhu, Hong Yang

This is the author's version of a work that has been accepted for publication in the Journal of Infrastructure Systems, Volume 23, Issue 4 (December 2017). The final version can be found at [doi.org/10.1061/\(ASCE\)IS.1943-555X.0000369](https://doi.org/10.1061/(ASCE)IS.1943-555X.0000369).

1
2 **Evacuation Zone Modeling under Climate Change:**
3 **A Data-Driven Method**
4

5
6 Kun Xie¹, Kaan Ozbay², Yuan Zhu³, Hong Yang⁴
7
8

9 **ABSTRACT**

10 Pre-determined evacuation zones can be used to estimate the demand of evacuees, which
11 is helpful in assessing the resilience of transportation systems in the presence of natural
12 disasters. Evacuation zones defined based on current road networks, environmental and
13 demo-economic characteristics of a region cannot remain the same in the future, since the
14 long-term climate change such as the rise of sea level would have major impacts on
15 hurricane-related risks. Traditional methods for the prediction of future evacuation zones
16 rely heavily on the storm surge models and could be time-consuming and costly to use.
17 This study develops a novel grid cell-based data-driven method which can predict future
18 evacuation zones under climate change without running the expensive storm surge models.
19 The map of Manhattan, which is the central area of New York City (NYC), was uniformly
20 split into 45×45 m² grid cells as the basic geographical units of analysis. A decision tree
21 and a random forest were used to capture the relationship between grid cell-specific
22 features such as geographical features, evacuation mobility, and demo-economic features
23 and current zone categories which could reflect the risk levels during hurricanes. Ten-fold

¹ Corresponding author, Department of Civil and Urban Engineering, Center for Urban Science and Progress, New York University, Brooklyn, NY 11201, USA. E-mail: kun.xie@nyu.edu

² Department of Civil and Urban Engineering, Center for Urban Science and Progress, New York University, Brooklyn, NY 11201, USA. E-mail: kaan.ozbay@nyu.edu

³ Department of Civil and Urban Engineering, Center for Urban Science and Progress, New York University, Brooklyn, NY 11201, USA. E-mail: yuan.zhu@nyu.edu

⁴ Department of Modeling, Simulation & Visualization Engineering, Old Dominion University, Norfolk, VA 23529, USA. E-mail: hyang@nyu.edu

24 cross-validation was used to evaluate model performance and it was found that the random
25 forest outperformed the decision tree in term of the accuracy and Kappa statistic. The
26 random forest was used to predict the delineation of evacuation zones in the 2050s and
27 2090s, based on the predicted sea level rises and changes of demo-economic features.
28 Compared with the current zoning, the areas with need of evacuation are expected to
29 expand in the future. The proposed method can be used to promptly estimate the future
30 evacuation zones under different sea level rise scenarios and can provide the convenience
31 to assess transportation system resilience in the context of climate change.

32

33 **Keywords:** Evacuation Zone, Emergency Management, Resilience, Random Forest,
34 Hurricane, Climate Change

35 INTRODUCTION

36 Hurricanes can devastate coastal areas with flooding, high wind, and rainfall, resulting in
37 serious loss of lives and property. It is important for emergency planners to define
38 evacuation zones which can indicate inhabitants whether or not they are prone to hurricane-
39 related risk in advance of disaster impacts. Pre-determined evacuation zones can be used to
40 estimate the demand of evacuees, which is helpful in assessing the resilience of
41 transportation systems. The term resilience has been used in a variety of domains ranging
42 from ecology to infrastructures systems (Ayyub 2014; Francis and Bekera 2014; Holling
43 1973; Linkov et al. 2014; Park et al. 2013; Vugrin et al. 2011). In this study, resilience is
44 defined as the ability of the transportation systems to maintain certain level of service under
45 hurricane evacuation scenarios. Similar definition can be seen in Heaslip et al. (2010), and
46 this definition reflects the absorptive capacity - the degree to which a system can mitigate
47 the impact of adverse events - of systems, which is one of three pillar resilience capacities
48 as stated in Francis and Bekera (2014). Since the long-term climate change could have
49 major impact on hurricane-related risks, evacuation zones defined based on current
50 network, environmental and socio-economic characteristics of a region cannot remain the
51 same in the future. One notable factor of climate change is global warming and the resulting
52 rise of sea level. According to the study of the United States Geological Survey in 2012,
53 the sea level of the Atlantic coast of North American rose by 1.97–3.80 mm per year
54 since 1990 (Sallenger Jr et al. 2012). The rise of sea level in the future is likely to promote
55 the flooding risk for coastal areas. Therefore, it is essential to consider the impact of climate
56 change on evacuation zone determination when evaluating the transportation system
57 resilience.

81 km of coastline and almost 3 million people living in the areas at the risk of hurricanes
82 (Gregory 2013). Considering the larger number of vulnerable coastal population, it is
83 essential to define up-to-date evacuation zones for the development of detailed evacuation
84 plan. Hurricane Sandy, which made landfall in October 2012 and is the second-costliest
85 hurricane in United States history (Xie et al. 2015), provides us valuable data to study.

86 This study focuses on the prediction of future evacuation zones in the context of
87 climate change. To predict future evacuation zones, traditional methods rely on the
88 estimation of surge flooding using models such as the SLOSH model and the ADCIRC (a
89 parallel advanced circulation model for oceanic, coastal, and estuarine waters) model
90 (Wilmot and Meduri 2005). However, the implementation of the SLOSH and ADCIRC
91 models can be really time-consuming and costly. For example, multiple runs of the SLOSH
92 model need to be executed to determine the maximum water elevation under scenarios with
93 different land fall points and storm intensities (Wilmot and Meduri 2005). Thereby, we
94 propose a novel data-driven method that can predict future evacuation zones under
95 different climate change scenarios, without running expensive storm surge simulations.
96 Machine learning algorithms are used to establish the relationship between current pre-
97 determined evacuation zones and hurricane-related factors, and then to predict how those
98 zones should be updated as those hurricane-related factors change in the future. Moreover,
99 a special consideration is given to the socio-economic factors such as the disability and
100 poverty, since communities with more vulnerable populations are known to be at higher
101 risk when confronting hurricanes.

102

103

104 **LITERATURE REVIEW**

105 Evacuation planning is a thematic research topic, particularly after a number of natural
106 disasters such as recent hurricanes Irene and Sandy on the east coast. There have been a
107 large number of research studies on related issues such as shelter location, transportation
108 routing and medical service in evacuation planning. However, only a limited number of
109 studies are available on the determination of evacuation zones.

110 Generally, hurricane evacuation zones are determined based on the risk of flooding.
111 Wilmot and Meduri (2005) and Meduri (2004) are among the early studies to develop a
112 detailed procedure to delineate hurricane evacuation zones using TransCAD. In the method
113 they proposed, basic zones of evacuation were created based on the key geographic
114 information system (GIS) data including a ground elevation layer, a zip code boundary
115 layer, and land use data. The SLOSH model was used to estimate the storm surge elevations
116 in the study area. The depth of inundation was estimated by subtracting the ground
117 elevation from the predicted surge height in each zone. Their proposed procedure was
118 demonstrated through a case on identifying the hurricane evacuation zones in the New
119 Orleans metropolitan area.

120 FRPC (2012) identified the evacuation zones in South Florida region according to
121 factors such as storm tide limits, wind vulnerability, population at risk, and flood prone
122 areas (based on 100-year flood zones).

123 When PBS&J were conducting hurricane evacuation studies in several states
124 (PBS&J 2007a; PBS&J 2007b), the evacuation zones were determined based on the surge
125 inundation limits developed by the US Army Corps of Engineers (USACE) using the
126 SLOSH model. The limits for category 1 through 4 tropical cyclones and the boundaries

127 of the minor civil divisions within each country were used to develop the evacuation zones
128 for various storm scenarios.

129 Other than hurricane evacuation zones, the National Tsunami Hazard Mitigation
130 Program (NTHMP) (NTHMP 2011) provide some guidelines and best practices for
131 tsunami evacuation mapping. It suggests that the evacuation mapping should consider
132 historical inundation information, select reasonable elevation based on local topography,
133 tectonic setting, and distance from local shorelines, interpolate and extrapolate inundation
134 based on estimated models. In case of no other tsunami hazard information and hurricane
135 storm surge maps, the Storm Surge Atlas Maps in consultation with the NTHMP scientific
136 representative was suggested for tsunami evacuation planning.

137 Similarly, the practices in Hawaii also provide some valuable experience in
138 evaluating and adjusting evacuation zones. For example, Mader (2010) modeled the hazard
139 of the evacuation zones in Hawaii based on the potential tsunami events. According to the
140 study, both elevation criteria and the Fritz criteria generalized from the surveys were used
141 to check the current evacuation zones in Hawaii (Liu et al. 2005; Mader 2010). The Fritz
142 criteria that defined the evacuation zones are: “(a) areas below 15 m above sea level and
143 within 0.4 km of shoreline or along rivers; (b) areas below 10 m above sea level and within
144 1.6 km of shoreline or along rivers; and (c) areas below 5 m above sea level and within 4.8
145 km of shoreline”. Similarly, in order to update the current evacuation zone maps developed
146 in the 1980s, the Fritz criteria have also been used by Meadows (2013) when comparing 3
147 potential new tsunami evacuation zone delineations for Hawaii.

148 All the aforementioned studies delineated the evacuations zones based on
149 hydrogeological and / or geographical features such as elevation, surge inundation, and the

150 distance to the shorelines. There are a number of studies exploring the demo-economic
151 factors that put residents at high risk when confronting natural disasters. Zoraster (2010)
152 reviewed 228 articles on vulnerable populations during hurricanes. He summarized risk
153 factors to be considered when planning for disaster preparation, which include poverty,
154 home ownership, poor English language proficiency, ethnic minorities, immigrant status,
155 and high-density housing. Morrow (1999) investigated the examples from Hurricane
156 Andrew and found that “the poor, the elderly, women-headed households and recent
157 residents, are at greater risk throughout the disaster response process”. Chakraborty et al.
158 (2005) used both geophysical risk and social vulnerability indices to assist the development
159 of evacuation strategies. The social vulnerability index is related to factors such as total
160 population, number of mobile homes, population below poverty level, children, the elderly,
161 and population with disabilities. Various studies (Chakraborty et al. 2005; Eldar 1992;
162 McGuire et al. 2007; Ortíz et al. 1986; Rizzo 1977; Sommer and Mosley 1972) suggested
163 that elderly persons and children are more vulnerable to the safety and health hazards of
164 natural disasters. The cut-off ages for defining the elderly differ from 60 (Rizzo 1977;
165 Sommer and Mosley 1972), to 65 (McGuire et al. 2007; Ortíz et al. 1986) and to 85
166 (Chakraborty et al. 2005). Similarly, cut-off ages for defining children differ from 5
167 (Chakraborty et al. 2005) to 9 (Rizzo 1977; Sommer and Mosley 1972). In this study, we
168 don’t use the cut-off ages to define the elderly and children. Instead of doing that, the
169 populations in seven different age groups (0-4, 5-9, 10-14, 60-64, 65-74, 75-84, and 85+)
170 are used as predictors in the evacuation zone prediction model, and the relationship
171 between different age groups and hurricane-related risk could be established automatically
172 by the proposed machine learning methods.

173 Most previous studies on evacuation zoning focus heavily on the implementation
174 of storm surge models. Evacuation zoning is mainly determined by the flooding risk and
175 less consideration is given to other risk factors such as evacuation mobility and demo-
176 economic features. This study aims to use machine learning methods to capture the
177 relationship between evacuation zoning and various hurricane-related factors. The
178 delineation of future hurricane evacuation zones can be estimated even if the outputs from
179 the storm surge models are unavailable. The effects of vulnerable populations such as are
180 accounted for in the proposed evacuation zoning models.

181

182 **DATA PREPARATION**

183 The map of Manhattan was uniformly split into a total of 25,440 grid cells with size of
184 45×45 m² as the basic geographical units of analysis. The selection of cell size is a trade-
185 off between information precision and computation cost. The width of a standard block in
186 Manhattan is about 90 m and the length of it is about 270 m (both are divisible by 45 m).
187 Using cells with lengths of 45 m can capture cell-specific features more precisely and can
188 provide street-by-street resolution for evacuation management. Zone category,
189 geographical features (e.g. average elevation above sea level), evacuation mobility (e.g.
190 distance to the nearest subway station) and demo-economic features (e.g. total population
191 and population with disability) were obtained for each cell using spatial analysis tools of
192 ArcGIS (Johnston et al. 2001). Detailed description on data collection will be presented in
193 the following paragraphs.

194 The NYC Hurricane Evacuation Zones Map (<http://maps.nyc.gov/hurricane/>) was
195 updated in 2013 after Hurricane Sandy. The 2013 evacuations zones are listed from zone

196 1 to zone 6, from the highest risk to the lowest risk. Each grid cell was attached to its zone
197 category which could reflect the risk level during hurricanes. In this study, four-level zone
198 category is used as the response variable in the proposed machine learning methods, with
199 “E1” corresponding to NYC 2013 evacuation zone 1, “E2” corresponding to NYC 2013
200 evacuation zone 2 and zone 3, and “E3” corresponding to NYC 2013 evacuation zone 4,
201 zone 5 and zone 6, and “S” corresponding to the safe zone beyond the evacuation region.

202 Digital Elevation Model (DEM) data of NYC provides a representation of the
203 terrain with elevations above the ground in a regular raster form. The DEM data of
204 Manhattan was extracted from National Elevation Dataset (NED, <http://ned.usgs.gov/>)
205 developed by U.S. Geological Survey (USGS). The resolution of the DEM data is 1 arc
206 second (about 27 m) and the pixel values are elevations in feet based on North American
207 Vertical Datum of 1988 (NAD83). The average elevation which is associated with the
208 flooding risk was aggregated for each grid cell. Another geographic feature collected for
209 each cell is the distance to the coast, since areas closer to the coast are more likely to be
210 affected by the storm surges.

211 Evacuation mobility is related to the efficiency of pre-storm evacuation. NYC
212 Office of Emergency Management (OEM) offers shelters during hurricanes in evacuation
213 centers. The distance to the nearest evacuation center was computed for each grid cell of
214 the map. Additionally, transportation mobility such as the distance to the nearest subway
215 station, the distance to the nearest bus stop and the distance to the nearest highway were
216 also obtained by using spatial tools of ArcGIS (Johnston et al. 2001).

217 In addition to evacuation mobility, demo-economic features can affect the division
218 of evacuation zones. For example, the total population is related with the priority of

219 evacuation, and the zones with large number of disables, elderlies, and children tend to be
220 more vulnerable. Twelve demo-economic features for each census tract were obtained from
221 the U.S. Census Bureau (<http://factfinder.census.gov>)

222 The descriptive statistics of predictors including geographic features, evacuation
223 mobility and demo-economic features are presented in Table 1. The spatial distributions of
224 those predictors are demonstrated in Fig. 2.

225

226 <Insert Figure Here>

227 **Fig. 2.** Spatial distributions of predictor

228

229

230 **METHODOLOGY**

231 In this section, we introduce classification tree and random forest models which can be
232 used to explore the pattern of evacuation zoning by using zone category as the response
233 variable and geographic features, evacuation mobility and demo-economic features as
234 predictors. Statistic measures for performance and cross-validation method are also
235 introduced in this section.

236

237 **Classification Tree and Random Forest**

238 A classification tree classifies observations by reclusively partitioning the predictor space
239 (Breiman et al. 1984). The classification tree is a non-parametric classifier, and hence no
240 assumption needs to be made on the form of relationship between the predictors and the
241 response variable. The classification tree is capable of capturing the nonlinear relationship
242 between the evacuation zone categories and relevant features. Additionally, the
243 classification tree is able to perform feature selection automatically by maximizing entropy

244 reduction (Breiman et al. 1984). The entropy for the node m is defined by the following
 245 equation (Quinlan 1986):

$$246 \quad Entropy_m = -\sum_{j=1}^J p_m^j \log_2 p_m^j \quad (1)$$

247 where J is the total number of classes and p_m^j is the proportion of the class j
 248 ($j=1,2,\dots,J$) on the node m . p_m^j can be obtained by:

$$249 \quad p_m^j = \frac{N_m^j}{N_m} \quad (2)$$

250 where N_m denotes the number of instances at the node m and N_m^j is the number of instances
 251 belong to the class j . The largest entropy on the node m is $\log_2 J$. If node m is not pure,
 252 it should be split to reduce the entropy. If $N_{m,p}$ of N_m take the branch p , the entropy after
 253 the split is given as:

$$254 \quad Entropy'_m = -\sum_{p=1}^P \frac{N_{m,p}}{N_m} \sum_{j=1}^J p_{m,p}^j \log_2 p_{m,p}^j \quad (3)$$

255 where P is the total number of branches and $p_{m,p}^j$ is the proportion of the class j on the
 256 branch p . $p_{m,p}^j$ is given by:

$$257 \quad p_{m,p}^j = \frac{N_{m,p}^j}{N_{m,p}} \quad (4)$$

258 where $N_{m,p}$ is the number of instances that take the branch p and $N_{m,p}^j$ is the number of
 259 instances that take the branch p and belong to the class j . The split that can maximize
 260 $Entropy_m - Entropy'_m$ is taken at the node m .

261 Let \mathbf{x}_i indicate a vector of predictors for the instance i ($i = 1, 2, \dots, N$, where N is
262 the sample size), y_i denote the category for the instance i . The algorithm for developing
263 a classification tree is as follows:

264 Step 1. Grow a large tree structure based on collected N samples and M
265 predictors. A recursive process is conducted by picking the best predictors from \mathbf{x}_i to
266 reduce the entropy.

267 Step 2. Prune the large tree to obtain subtrees ST_k ($k = 1, 2, \dots, K$, where K is the
268 total number of subtrees).

269 Step 3. Predict the category \hat{y}_i of the instance i using the subtrees ST_k in a cross-
270 validation setting. The accuracy of the subtrees ST_k is $\sum_i^N c_i / N$; where $c_i = 1$ when
271 $y_i = \hat{y}_i$, otherwise $c_i = 0$.

272 Step 4. Select the best tree model from the subtrees based on the prediction accuracy.

273 Despite its advantages, the classification tree is found to generate unstable
274 predictions given certain perturbations (Breiman 1996). To improve stability, Breiman
275 (2001) proposed the random forest method which constructs multiple classification trees
276 by bootstrapping (i.e. random sampling with replacement) the samples and employing
277 random feature selection. The random forest lets each individual tree vote for the predicted
278 class and uses the majority vote as the final output. The structure of the random forest is
279 demonstrated in Fig. 3. The algorithm for developing and evaluating a random forest is as
280 follows:

281 Step 1. Create a training subset b ($b=1,2,\dots,B$, where B is the predefined
 282 number of trees) by bootstrapping n samples from the whole training set with size N .

283 Step 2. Select m predictors at random from M predictors collected.

284 Step 3. Grow a classification tree T_b based on selected n samples and m predictors
 285 in Steps 1 and 2. Obtain the predicted categories $T_b(\mathbf{x}_i)$ for each instance.

286 Step 4: Repeat Steps 1-3 for B times.

287 Step 5: Predict the category \hat{y}_i for the instance i using the mode of the set
 288 $\{T_b(\mathbf{x}_i) | b = 1, 2, \dots, B\}$.

289 Step 6: The accuracy of the random forest is $\sum_i^N c_i / N$; where $c_i = 1$ when $y_i = \hat{y}_i$,
 290 otherwise $c_i = 0$.

291 The random forest has been widely used in natural disaster management recently
 292 (Guikema et al. 2014; Nateghi et al. 2014; Staid et al. 2014; Wanik et al. 2015). Via
 293 selecting samples and features randomly and integrating outcomes of individual trees, the
 294 random forest is more robust with respect to noises. This noise robustness is essential in
 295 cell-based projection of evacuation zones in the presence of noisy data.

296

297 <Insert Figure Here>

298 **Fig. 3.** A structure demonstration of the random forest model

299 **Model Assessment**

300 Classification accuracy is widely used as a statistical measure of the extent to which the
 301 proposed classification tree and random forest perform. The accuracy can be simply

302 computed by using the number of correctly classified instances divided by the total number
303 of instances. However, using the accuracy as the only performance indicator can be
304 misleading. For example, in the case there is a large class imbalance, a model which always
305 predicts the majority class can achieve a high classification accuracy, but is not useful in
306 the problem domain.

307 As an alternative to accuracy, Kappa statistic corrects for the potential biases caused
308 by class imbalance. Kappa statistic is computed based on the difference between the
309 observed agreement and the expected agreement obtained by random guess (Viera and
310 Garrett 2005):

311

$$312 \quad K = \frac{P_0 - P_c}{1 - P_c} \quad (5)$$

313 where P_0 is the proportion of observed agreements and P_c is the proportion of agreements
314 expected by chance. The Kappa statistic lie on a -1 to 1 scale, where 1 is the best agreement,
315 0 is what would be expected by chance and -1 is the worst agreement. According to Landis
316 and Koch (1977), the magnitude of the Kappa statistic can be interpreted as: -1~0 = poor,
317 0.01~0.20 = slight, 0.21~0.40 = fair, 0.41~0.60 = moderate, 0.61~0.80 = substantial, and
318 0.81~1 = almost perfect.

319 To compare the predictive performance of different algorithms, a ten-fold cross-
320 validation was performed in this study. The total dataset was split into 10 subsets randomly,
321 and each of them was repeatedly left out as the validation set while the rest was used for
322 training. The final accuracy and Kappa statistic were the combinations of outcomes when

323 using each validation set for model assessment. The cross-validation can properly address
324 the over-fitting issues.

325 **MODELING RESULTS**

326 The proposed classification tree and random forest were used to estimate evacuation zone
327 categories based on the geographic features, evacuation mobility and demo-economic
328 features. Open source software, Weka, was used to estimate the classification trees and
329 random forests (Hall et al. 2009). A ten-folder cross-validation was performed to obtain
330 accuracies and Kappa statistics. The selection of parameters in the classification tree and
331 the random forest can have impacts on model outcomes. We tested a variety of parameter
332 sets and selected the best combination based on model performance and convergence time.
333 The parameters selected are summarized in Table 2.

334 Performance measures of the classification tree and the random forest are reported
335 in Table 3. For comparison purpose, the performance measures of other commonly used
336 machine learning methods including the logistic regression (Hosmer Jr and Lemeshow
337 2004), the support vector machine (SVM) (Cortes and Vapnik 1995) and the neural
338 network (Hagan et al. 1996) are also presented. According to Table 3, both the
339 classification tree and the random forest can result in higher accuracies than other machine
340 learning methods and “almost perfect” Kappa statistics which are greater than 0.8. When
341 comparing their performance, the random forest can yield higher accuracy than that of the
342 classification tree (95.69% vs 91.95%). In addition, the higher value of Kappa statistic of
343 the random forest provides additional evidence that the random forest has a better
344 predictive performance.

345 To have a detailed evaluation of the predictive performance, the confusion matrices
346 of the classification tree and the random forest are reported in Table 4 (a) and (b),
347 respectively. For each zone category, the random forest results in more correctly classified
348 instances than the classification tree does. For example, the random forest identifies 1,880
349 cells in the E1 zone correctly, which is greater than the number 1,745 by using the
350 classification tree. Additionally, according to Table 4 (a), the random forest can output a
351 really accurate prediction for each zone category. Only 13 cells out of 1,988 in E1 zone
352 with high risk are classified as belong to safe zone, and only 7 cells out of 13,823 in the
353 safe zone are regarded to be in the risky E1 zone.

354 Regarding the better performance, the prediction outcomes of the random forest are
355 visualized in the GIS map and compared with actual evacuation zones as presented in Fig.
356 4. It is found that the estimated evacuation zone division is quite similar to the actual one.
357 It implies that the random forest succeeds in learning the potential pattern of delineating
358 zones with different risk levels. However, it is likely that the same random forest developed
359 for Manhattan couldn't achieve the same prediction accuracy for other regions, since the
360 relationship between zone categories and risk factors are location-specific. The effects of
361 predictors such as the distance to the coast and average elevation on flooding risks can vary
362 greatly when confronting totally different hydrogeological environments in other regions.
363 It is highly recommended to re-estimate the random forest models to capture the local
364 characteristics of other coastal regions vulnerable to hurricanes and future effects of
365 climate change.

366

367

<Insert Figure Here>

368 **Fig. 4.** Current evacuation zones (left) and predicted evacuation zones using the random
369 forest (right)

370

371 **PREDICTION OF FUTURE EVACUATION ZONES**

372 The main climate change which would have a great impact on the evacuation zoning is the
373 sea level rise. The propose method can be used to promptly predict evacuation zones under
374 different scenarios of sea level rises. As an example, this paper uses the sea level
375 projections of the work reported in Zhang et al. (2014), which is a part of the New York
376 State Resiliency Institute for Storms & Emergencies (NYRISE) project. In their study, two
377 greenhouse gas emission scenarios are used to predict future sea level rise including the
378 Representative Concentration Pathway (RCP) 4.5 (Thomson et al. 2011) and RCP 8.5 (Van
379 Vuuren et al. 2011). In the RCP 4.5 scenario where countries work together to combat
380 climate change, the climate radiative forcing to the atmosphere from anthropogenic
381 emissions is 4.5 watts per square meter over the globe. The RCP 8.5 scenario assumes that
382 little coordinated actions are made among countries, so that the climate radiative forcing
383 to the atmosphere from anthropogenic emissions is as high as 8.5 watts per square meter
384 over the globe.

385 Zhang et al. (2014) used a component-by-component analysis (Slangen et al. 2012)
386 to project future sea level rises. The main components affecting sea level include global
387 thermal expansion, local changes in ocean height, loss of ice from Greenland and Antarctic
388 ice sheets, land water storage, etc. The future sea levels are forecasted under the “business
389 as usual” emission scenario RCP 8.5. The upper 95% bounds of sea levels are estimated to
390 be 0.92 m for the 2050s and 1.14 m for the 2090s. As a result of climate change, the terrain

391 elevation above the sea level is expected to decrease. This will lead to a higher flooding
392 risk and thus the evacuation zone categories need to be updated accordingly.

393 The change of demo-economic features is taken into consideration as well. Table 5
394 presents the population growth rate by age group. The projected growth rate for the whole
395 population in Manhattan is 2.17% per ten years. Population decline is only observed for
396 the age group 60~64. It is worth mentioning that the population over 85 have the highest
397 growth rate 16.78%, which would increase the hurricane-related vulnerability. The total
398 population and the populations in different age groups in the 2050s and the 2090s were
399 predicted based on the assumption that the growth rates listed in Table 5 stay constant.
400 Population below the poverty level, population not covered by health insurance, population
401 with disability and population who are not proficient in English in the 2050s and the 2090s
402 were predicted use the grow rate for the whole population in Manhattan (2.17%).

403 The proposed random forest is used to predict the evacuation zones for the 2050s
404 and 2090s, based on the expected decrease in average elevation above the sea level, the
405 changes in demo-economic features and the assumption that evacuation mobility is kept
406 the same the future. The predicted future evacuation zones are presented in Fig. 5
407 Compared with the current zoning in Fig. 4, the areas with need of evacuation are expected
408 to expand in the future. Despite the good performance of the random forest, it is inevitable
409 to have prediction errors. A procedure to modify evacuation zones manually is suggested.
410 Some principles are suggested to guide the modification of evacuation zones. For example,
411 one type of evacuation zone may not be established within another. Also, some
412 consideration should been given to the identifiable features of zoning (Wilmot and Meduri
413 2005).

414 <Insert Figure Here>

415 **Fig. 5.** Predicted evacuation zones for the 2050s (left) and the 2090s (right)

416 Comparisons of the current evacuation zones with the predicted evacuation zones
417 for the 2050s and the 2090s are presented in Table 6. In the 2050s, the areas of the E1, E2
418 and E3 categories are expected to increase by 11.07% and 10.71% and 3.10%, respectively,
419 compared with the current zone division; whereas the areas of the S category are expected
420 to decrease by 5.33%. Similarly, in the 2090s, 15.95% more area of the E1 category, 4.94%
421 more area of the E2 category, 5.83% more area of the E3 category and 6.09% less area of
422 the S category are predicted. Projected evacuation zone divisions can be used by
423 emergency managers to estimate evacuation demand in the future. Knowing the evacuation
424 demand can be helpful in developing effective evacuation plans such as time to start
425 evacuation and selection of evacuation routes, and in managing emergency resources such
426 as determining the number of shelters, food and medicines provided to evacuees.

427

428 **SUMMARY AND CONCLUSIONS**

429 This study develops a novel data-driven method to predict the division of future evacuation
430 zones in the context of climate change, which is an essential input to estimate the resilience
431 of transportation systems. The map of Manhattan was uniformly split into 45×45 m² grid
432 cells as the basic geographical units of analysis. Evacuation zone category (E1, E2, E3 and
433 S), geographical features (including average elevation above sea level and distance to
434 coast), evacuation mobility (including distance to the nearest evacuation center, distance
435 to the nearest subway station, distance to the nearest bus stop and distance to the nearest
436 expressway), and demo-economic features (including total population, population below

437 the poverty level, and population with disability) in the current year were captured for each
438 cell. The future sea level rises estimated by Zhang et al. (2014) were used as an example
439 to predict future evacuation zones. As a result of sea level rises, the average elevation above
440 sea level is predicted to decrease and storm-related risk for the same region is likely to be
441 higher in the future. Various machine learning methods were trained to relate cell-specific
442 features with current zone categories which could reflect the risk levels during storms. Ten-
443 fold cross-validation was used to evaluate model performance and it was found that the
444 random forest outperformed the others in term of the accuracy and Kappa statistic. The
445 random forest was used to predict the delineation of evacuation zones in the 2050s and
446 2090s, based on the predicted sea level rises and changes of demo-economic features.
447 Compared with the current zoning, the areas with need of evacuation are expected to
448 expand in the future.

449 A practical usage of our integrated methodology is that it combines the zoning
450 model with the climate model to determine the change in evacuation zones in response to
451 climate variability. The proposed data-driven method can be used to promptly estimate the
452 evacuation zones under different sea level rise scenarios, without running storm surge
453 simulations which are generally time-consuming and costly. Transportation system
454 resilience in the context of climate change can be estimated based on the projected zonings
455 under different scenarios. The proposed method can support decision-making in the
456 evacuation planning and the management of emergency resources. For example, if the
457 demand of evacuees increases dramatically in scenarios with sea level rises, it could take
458 longer time to evacuate the residents prone to the hurricane-related risks, and thus the
459 evacuation process should be started earlier. Also, the number of shelters, the amount of

460 food and medicine stocked in evacuation centers are closely related to the demand of
461 evacuees predicted. Thus, our results in this paper can be used to develop various realistic
462 planning and training scenarios that reflect the impact of the predicted changes of
463 evacuation zoning.

464 Despite the great performance of the random forest, domain experts are still needed
465 to make the final decision about the size and type of evacuation zones. But we hope that
466 the methodology proposed in this paper will provide them with additional insights. For
467 future work, the study area will be expanded from Manhattan to the whole New York
468 metropolitan area. An estimation of the number of residents to be evacuated in a larger
469 region can be obtained. Additional work is needed to predict the future variation of
470 evacuation mobility and demo-economic features, since they are closely related to the
471 division of evacuation zones. Travel time could be used instead of travel distance as the
472 metrics to represent evacuation mobility. In addition, evacuation simulation under different
473 sea level rise scenarios will be conducted and level of services under those scenarios will
474 be estimated to assess the resilience of transportation systems.

475

476 **ACKNOWLEDGMENTS**

477 The work is partially funded by New York State Resiliency Institute for Storms &
478 Emergencies (NYRISE) and CitySMART laboratory at New York University. The authors
479 would like to thank Prof. Minghua Zhang and his team from the State University of New
480 York at Stony Brook for providing the climate prediction data as a part of the NYRISE
481 project. The authors also thank the anonymous reviewers for their valuable comments and
482 suggestions that help improve the paper. The contents of this paper reflect views of the

483 authors who are responsible for the facts and accuracy of the data presented herein. The
 484 contents of the paper do not necessarily reflect the official views or policies of the agencies.

485

486 **REFERENCES**

- 487 Ayyub, B. M. (2014). "Systems resilience for multihazard environments: Definition,
 488 metrics, and valuation for decision making." *Risk Analysis*, 34(2), 340-355.
- 489 Bloomberg, M. R., and Burden, A. M. (2013). "New York City Population Projections by
 490 Age/Sex & Borough, 2010-2040." New York City.
- 491 Breiman, L. (1996). "Bagging predictors." *Machine learning*, 24(2), 123-140.
- 492 Breiman, L. (2001). "Random forests." *Machine learning*, 45(1), 5-32.
- 493 Breiman, L., Friedman, J., Stone, C. J., and Olshen, R. A. (1984). *Classification and*
 494 *regression trees*, CRC press.
- 495 Chakraborty, J., Tobin, G. A., and Montz, B. E. (2005). "Population evacuation:
 496 assessing spatial variability in geophysical risk and social vulnerability to natural
 497 hazards." *Natural Hazards Review*, 6(1), 23-33.
- 498 Cortes, C., and Vapnik, V. (1995). "Support-vector networks." *Machine learning*, 20(3),
 499 273-297.
- 500 Eldar, R. (1992). "The needs of elderly persons in natural disasters: observations and
 501 recommendations." *Disasters*, 16(4), 355-358.
- 502 Francis, R., and Bekera, B. (2014). "A metric and frameworks for resilience analysis of
 503 engineered and infrastructure systems." *Reliability Engineering & System Safety*,
 504 121, 90-103.
- 505 FRPC (2012). "Florida Statewide Regional Evacuation Study Program." *Regional*
 506 *Population and Vulnerability Analysis* <http://www.sfrpc.com/sresp.htm>.
- 507 Gregory, K. (2013). "City Adds 600,000 People to Storm Evacuation Zones."
 508 [http://www.nytimes.com/2013/06/19/nyregion/new-storm-evacuation-zones-](http://www.nytimes.com/2013/06/19/nyregion/new-storm-evacuation-zones-add-600000-city-residents.html)
 509 [add-600000-city-residents.html](http://www.nytimes.com/2013/06/19/nyregion/new-storm-evacuation-zones-add-600000-city-residents.html)>. (07/21/2015).
- 510 Guikema, S. D., Nateghi, R., Quiring, S. M., Staid, A., Reilly, A. C., and Gao, M. (2014).
 511 "Predicting hurricane power outages to support storm response planning." *IEEE*
 512 *Access*, 2, 1364-1373.
- 513 Hagan, M. T., Demuth, H. B., Beale, M. H., and De Jesús, O. (1996). *Neural network*
 514 *design*, PWS publishing company Boston.
- 515 Hall, M., Frank, E., Holmes, G., Pfahringer, B., Reutemann, P., and Witten, I. H. (2009).
 516 "The WEKA data mining software: an update." *ACM SIGKDD explorations*
 517 *newsletter*, 11(1), 10-18.
- 518 Heaslip, K., Louisell, W., Collura, J., and Urena Serulle, N. (2010). "A sketch level
 519 method for assessing transportation network resiliency to natural disasters and
 520 man-made events."
- 521 Holling, C. S. (1973). "Resilience and stability of ecological systems." *Annual review of*
 522 *ecology and systematics*, 1-23.
- 523 Hosmer Jr, D. W., and Lemeshow, S. (2004). *Applied logistic regression*, John Wiley &
 524 Sons.

- 525 Johnston, K., Ver Hoef, J. M., Krivoruchko, K., and Lucas, N. (2001). *Using ArcGIS*
526 *geostatistical analyst*, Esri Redlands.
- 527 Landis, J. R., and Koch, G. G. (1977). "The measurement of observer agreement for
528 categorical data." *biometrics*, 159-174.
- 529 Linkov, I., Bridges, T., Creutzig, F., Decker, J., Fox-Lent, C., Kröger, W., Lambert, J. H.,
530 Levermann, A., Montreuil, B., and Nathwani, J. (2014). "Changing the resilience
531 paradigm." *Nature Climate Change*, 4(6), 407-409.
- 532 Liu, P. L.-F., Lynett, P., Fernando, H., Jaffe, B. E., Fritz, H., Higman, B., Morton, R.,
533 Goff, J., and Synolakis, C. (2005). "Observations by the International Tsunami
534 Survey Team in Sri Lanka." *Science*, 308(June), 1595.
- 535 Mader, C. L. "Tsunami Hazard to Hawaii from a M9+ Event Similar to 2004 Indian
536 Ocean Tsunami." *Proc., Pacific Congress on Marine Science and Technology,*
537 *PACON 2010, June 1-5, 2010.*
- 538 McGuire, L. C., Ford, E. S., and Okoro, C. A. (2007). "Natural disasters and older US
539 adults with disabilities: implications for evacuation." *Disasters*, 31(1), 49-56.
- 540 Meadows, D. (2013). "A Comparison of 3 Potential New Tsunami Evacuation Zone
541 Criteria for Hawaii." *A Report to the Hawaii Technical Review Committee*
542 *Science Advisory Working Group*www.mccohi.com/tsunami/hihazard.pdf
543 (Accessed December 17, 2013).
- 544 Meduri, N. (2004). "Development of a Methodology to Delineate Hurricane Evacuation
545 Zones, Master's Thesis." Master of Science, Louisiana State University.
- 546 Morrow, B. H. (1999). "Identifying and mapping community vulnerability." *Disasters*,
547 23(1), 1-18.
- 548 Nateghi, R., Guikema, S. D., and Quiring, S. M. (2014). "Forecasting hurricane-induced
549 power outage durations." *Natural Hazards*, 74(3), 1795-1811.
- 550 NTHMP (2011). "Guidelines and Best Practices for Tsunami Evacuation Mapping
551 Guidelines." <http://nthmp.tsunami.gov/> (Accessed December 17, 2013).
- 552 NYC (2013). "Deputy mayor holloway and office of emergency management
553 commissioner Bruno announce final updated hurricane evacuation zones."
- 554 Ortíz, M. R., Roman, M. R., Latorre, A. V., and Soto, J. Z. (1986). "Brief description of
555 the effects on health of the earthquake of 3rd March 1985–Chile." *Disasters*,
556 10(2), 125-140.
- 557 Park, J., Seager, T. P., Rao, P. S. C., Convertino, M., and Linkov, I. (2013). "Integrating
558 risk and resilience approaches to catastrophe management in engineering
559 systems." *Risk Analysis*, 33(3), 356-367.
- 560 PBS&J (2007a). "Maine Hurricane Evacuation Study Transportation Analysis." Post,
561 Buckley, Schuh and Jernigan, Inc., Tallahassee, Florida.
- 562 PBS&J (2007b). "New Jersey Hurricane Evacuation Study Transportation Analysis." Post,
563 Buckley, Schuh and Jernigan, Inc., Tallahassee, Florida.
- 564 Quinlan, J. R. (1986). "Induction of decision trees." *Machine learning*, 1(1), 81-106.
- 565 Rizzo, B. G. L. (1977). "Earthquake injuries related to housing in a Guatemalan village."
566 *Science*, 197, 638-643.
- 567 Sallenger Jr, A. H., Doran, K. S., and Howd, P. A. (2012). "Hotspot of accelerated sea-
568 level rise on the Atlantic coast of North America." *Nature Climate Change*, 2(12),
569 884-888.

- 570 Slangen, A., Katsman, C., van de Wal, R., Vermeersen, L., and Riva, R. (2012).
 571 "Towards regional projections of twenty-first century sea-level change based on
 572 IPCC SRES scenarios." *Climate dynamics*, 38(5-6), 1191-1209.
- 573 Sommer, A., and Mosley, W. (1972). "East Bengal cyclone of November, 1970:
 574 epidemiological approach to disaster assessment." *The Lancet*, 299(7759), 1030-
 575 1036.
- 576 Staid, A., Guikema, S. D., Nateghi, R., Quiring, S. M., and Gao, M. Z. (2014).
 577 "Simulation of tropical cyclone impacts to the US power system under climate
 578 change scenarios." *Climatic Change*, 127(3-4), 535-546.
- 579 Thomson, A. M., Calvin, K. V., Smith, S. J., Kyle, G. P., Volke, A., Patel, P., Delgado-
 580 Arias, S., Bond-Lamberty, B., Wise, M. A., and Clarke, L. E. (2011). "RCP4. 5: a
 581 pathway for stabilization of radiative forcing by 2100." *Climatic Change*, 109(1-
 582 2), 77-94.
- 583 Van Vuuren, D. P., Edmonds, J., Kainuma, M., Riahi, K., Thomson, A., Hibbard, K.,
 584 Hurtt, G. C., Kram, T., Krey, V., and Lamarque, J.-F. (2011). "The representative
 585 concentration pathways: an overview." *Climatic Change*, 109, 5-31.
- 586 Viera, A. J., and Garrett, J. M. (2005). "Understanding interobserver agreement: the
 587 kappa statistic." *Fam Med*, 37(5), 360-363.
- 588 Vugrin, E. D., Warren, D. E., and Ehlen, M. A. (2011). "A resilience assessment
 589 framework for infrastructure and economic systems: Quantitative and qualitative
 590 resilience analysis of petrochemical supply chains to a hurricane." *Process Safety
 591 Progress*, 30(3), 280-290.
- 592 Wanik, D., Anagnostou, E., Hartman, B., Frediani, M., and Astitha, M. (2015). "Storm
 593 outage modeling for an electric distribution network in Northeastern USA."
 594 *Natural Hazards*, 79(2), 1359-1384.
- 595 Wilmot, C., and Meduri, N. (2005). "Methodology to establish hurricane evacuation
 596 zones." *Transportation Research Record: Journal of the Transportation Research
 597 Board*(1922), 129-137.
- 598 Xie, K., Ozbay, K., and Yang, H. (2015). "Spatial analysis of highway incident durations
 599 in the context of Hurricane Sandy." *Accident Analysis & Prevention*, 74, 77-86.
- 600 Yang, H., Morgul, E. F., Ozbay, K., and Xie, K. (2016). "Modeling Evacuation Behavior
 601 under Hurricane Conditions." *Transportation Research Record*.
- 602 Zhang, M., Bokuniewicz, H., Lin, W., Jang, S.-g., and Liu, P. (2014). "Climate Risk
 603 Report for Suffolk and Nassau."
- 604 Zhu, Y., Ozbay, K., Xie, K., Yang, H., and Morgul, E. F. "Network modeling of
 605 hurricane evacuation using data driven demand and incident induced capacity loss
 606 models." *Proc., Transportation Research Board, Washington, D.C.*
- 607 Zoraster, R. M. (2010). "Vulnerable populations: Hurricane Katrina as a case study."
 608 *Prehospital and disaster medicine*, 25(01), 74-78.

609

610

611

612

Table 1. Descriptive Statistics of Predictors (N = 25,440 Grid Cells)

Predictor	Mean	S.D.
Geographic feature		
Average elevation above sea level (m)	15.99	13.84
Distance to coast (m)	762.46	464.84
Evacuation mobility		
Distance to the nearest evacuation center (m)	1014.34	519.64
Distance to the nearest subway station (m)	352.19	222.05
Distance to the nearest bus stop (m)	104.86	91.50
Distance to the nearest expressway (m)	565.47	434.10
Demo-economic feature		
Total population	42.78	31.43
Population not covered by health insurance	6.54	6.82
Population below the poverty level	8.11	10.22
Population with disability	6.00	3.84
Population who are not proficient in English	9.60	13.81
Population aged 0-4	2.94	2.47
Population aged 5-9	1.85	1.68
Population aged 10-14	2.68	2.64
Population aged 60-64	3.24	2.56
Population aged 65-74	4.40	3.52
Population aged 75-84	2.59	2.42
Population aged 85 and over	1.17	1.25

Note: All the demo-economic features are indicating the number of people in specific groups.

615

Table 2. Parameter Selection for the Classification Tree and the Random Forest

Classification Tree	Random Forest
○ Prune trees: true	○ Maximum depth of the tree:
○ Confidence factor for pruning: 0.25	unlimited
○ Maximum depth of the tree:	○ Number of features randomly
unlimited	selected: $\log(M)+1$, where M is the
○ Minimum number of instances per	total predictor number
leaf: 10	○ Number of trees: 60

616

617

618 **Table 3.** Performance Measures of the Classification Tree and the Random Forest

	Logistic Regression	SVM	Neural Network	Classification Tree	Random Forest
Correctly classified instances	21582	21881	22784	23392	24342
Incorrectly classified instances	3858	3559	2656	2048	1098
Total number of instances	25440	25440	25440	25440	25440
Accuracy	84.83%	86.01%	89.56%	91.95%	95.69%
Kappa statistic	0.7537	0.7724	0.8292	0.8694	0.9299

619

620

621 **Table 4.** Confusion Matrix of the Classification Tree (a) and the Random Forest (b)

622 (a)

Decision Tree		Classified as				Total
		E1	E2	E3	S	
Actual zone category	E1	1,745	164	53	26	1,988
	E2	180	2,436	339	43	2,998
	E3	52	286	5,857	436	6,631
	S	33	47	389	13,354	13,823

623

624 (b)

Random Forest		Classified as				Total
		E1	E2	E3	S	
Actual zone category	E1	1,880	76	19	13	1,988
	E2	92	2,679	204	23	2,998
	E3	12	191	6,180	248	6,631
	S	7	22	191	13,603	13,823

625

626

627

Table 5. Population Growth Rate by Age Group

628

in Manhattan (Bloomberg and Burden 2013)

Age Group	Population in 2010	Predicted Population in 2040	Growth Rate /10 years
0-4	76,579	76,687	0.05%
5-9	61,323	66,801	2.89%
10-14	58,229	63,630	3.00%
60-64	85,574	82,682	-1.14%
65-74	115,369	131,655	4.50%
75-84	68,397	97,394	12.50%
85+	30,387	48,395	16.78%
Total Population	1,585,873	1,691,617	2.17%

629

630

631 **Table 6.** Comparisons of the Current Evacuation Zones with Predicted
 632 Evacuation Zones in the 2050s and the 2090s

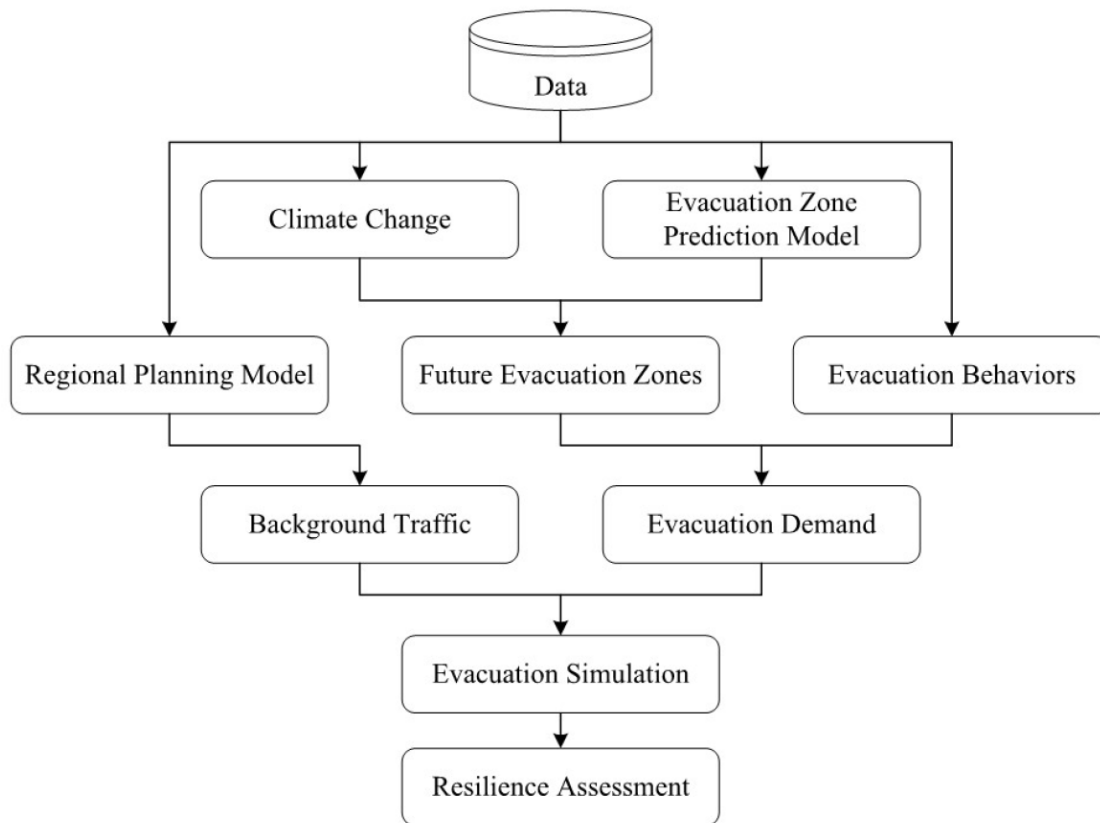
Zone Category	2050s		2090s	
	Cell	Percentage	Cell	Percentage
	Number	Change	Number	Change
E1 (current cell number=1,988)	2,208	11.07%	2,305	15.95%
E2 (current cell number=2,998)	3,319	10.71%	3,146	4.94%
E3 (current cell number=6,631)	6,827	3.10%	7,008	5.83%
S (current cell number=13,823)	13,086	-5.33%	12,981	-6.09%

633

634

635

Figure 1

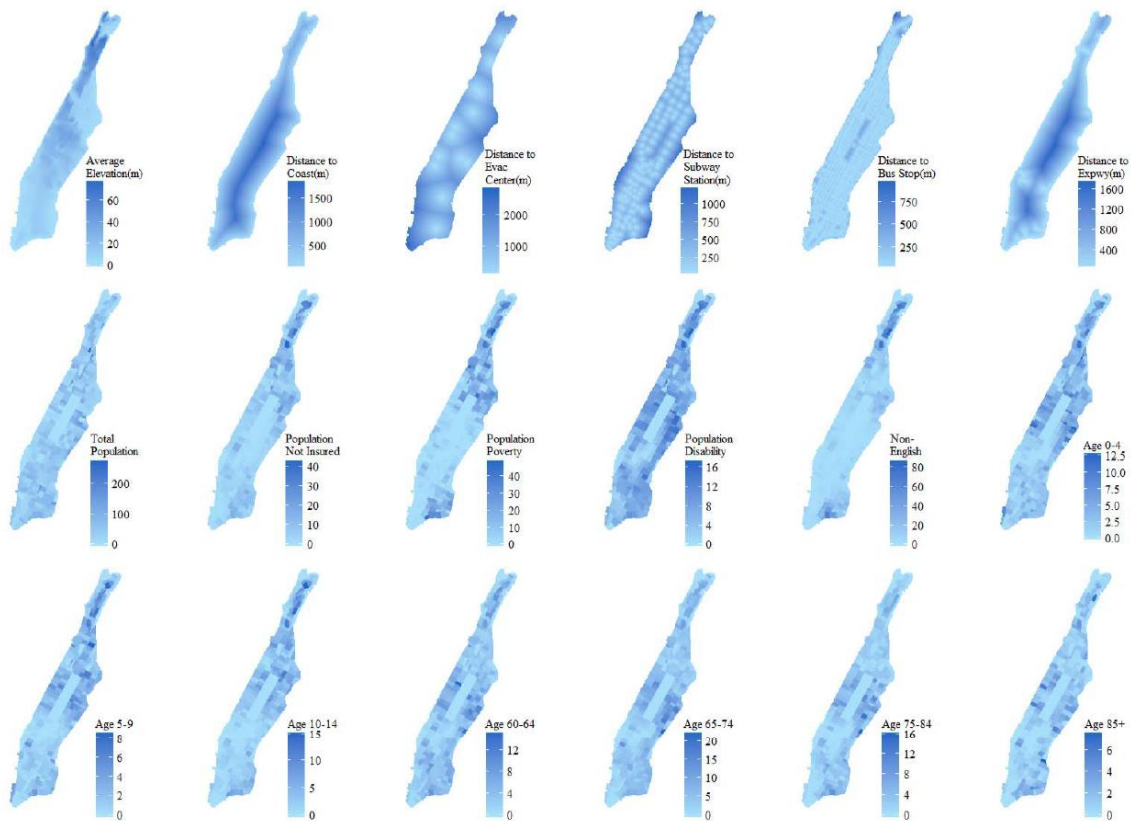


636

637

638

Figure 2

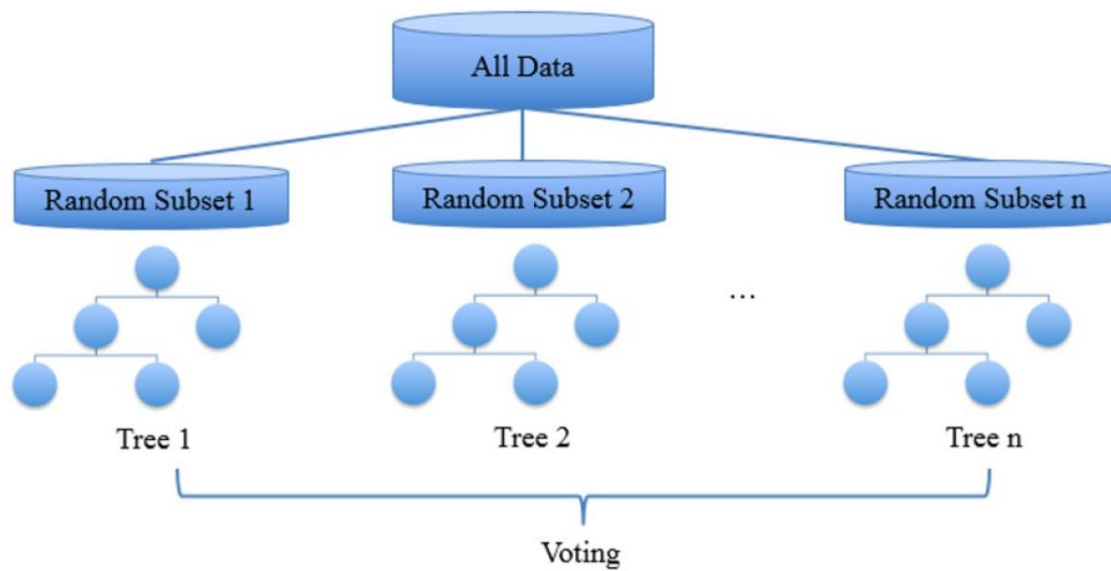


639

640

641

Figure 3

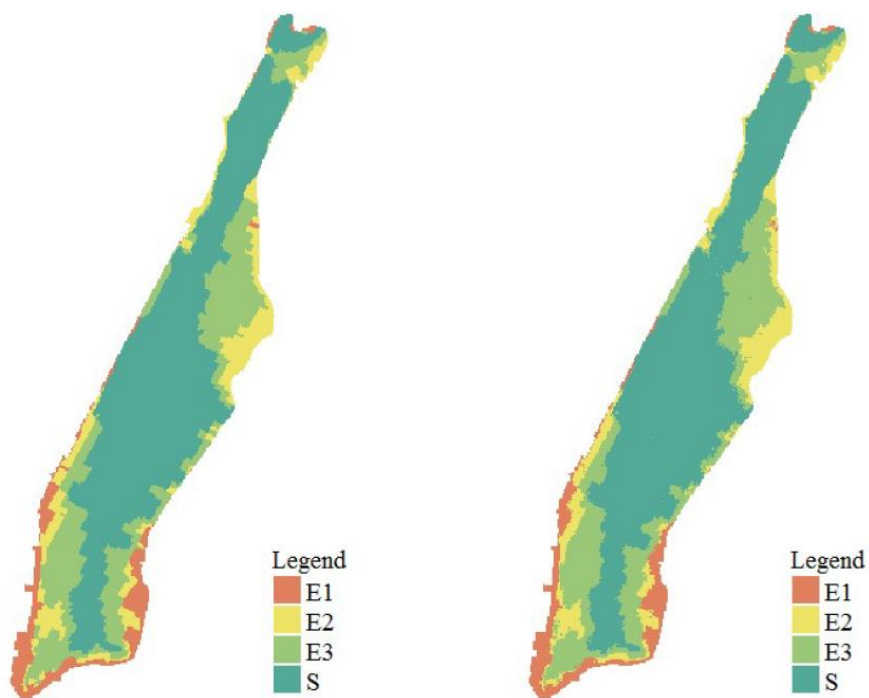


642

643

644

Figure 4

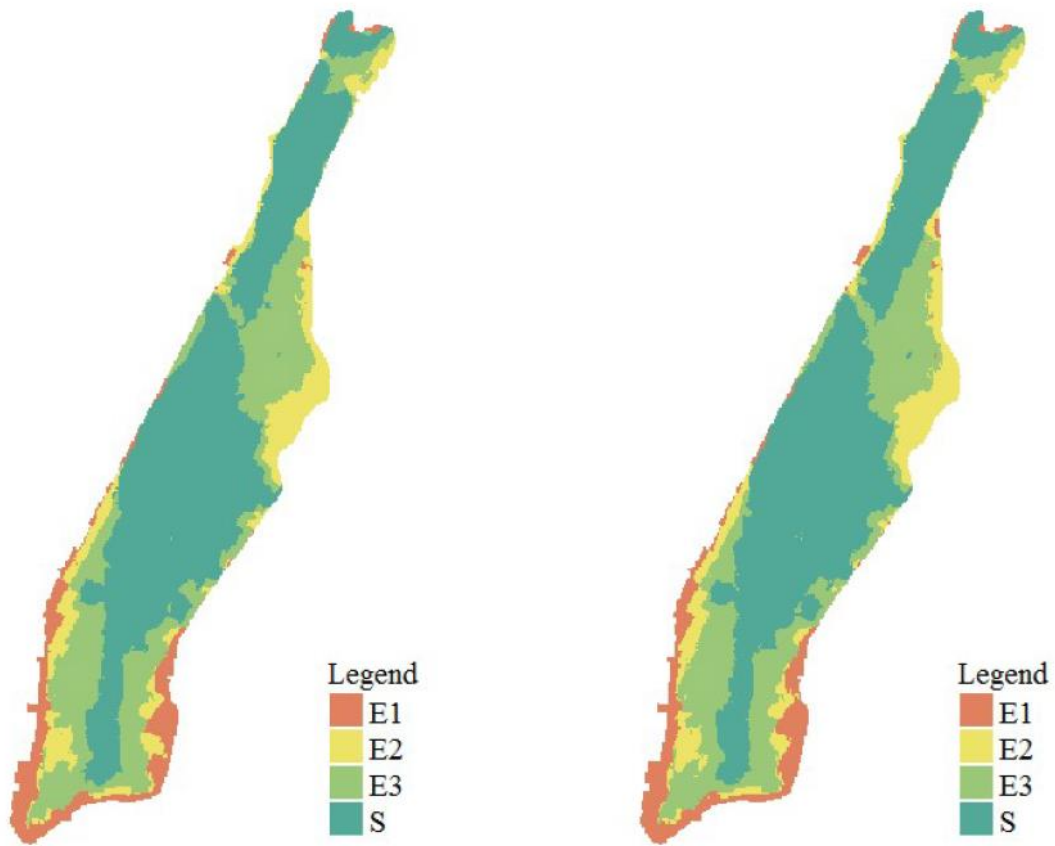


645

646

647

Figure 5



648